

Subdivision for Powell–Sabin Spline Surfaces

Evelyne Vanraes
Joris Windmolders
Adhemar Bultheel
Paul Dierckx

Report TW 345, September 2002



Katholieke Universiteit Leuven
Department of Computer Science

Celestijnenlaan 200A – B-3001 Heverlee (Belgium)

Subdivision for Powell–Sabin Spline Surfaces

Evelyne Vanraes
Joris Windmolders
Adhemar Bultheel
Paul Dierckx

Report TW 345, September 2002

Department of Computer Science, K.U.Leuven

Abstract

In this paper we present an algorithm for calculating the B-spline representation of a Powell–Sabin spline surface on a refinement of the given triangulation. The resulting subdivision scheme is a triadic scheme; every original edge is split into three new edges. The presented rules are derived using the fact that triadic subdivision can be seen as two steps of $\sqrt{3}$ -subdivision. The scheme is numerically stable and generally applicable, there are no restrictions on the initial triangulation.

Keywords : Powell–Sabin splines, subdivision, normalised B-splines, CAGD.
AMS(MOS) Classification : 65D07, 65D17, 68U07.

Subdivision for Powell–Sabin Spline Surfaces

Evelyn Vanraes, Joris Windmolders
Adhemar Bultheel, Paul Dierckx

September 2002

Abstract

In this paper we present an algorithm for calculating the B-spline representation of a Powell–Sabin spline surface on a refinement of the given triangulation. The resulting subdivision scheme is a triadic scheme; every original edge is split into three new edges. The presented rules are derived using the fact that triadic subdivision can be seen as two steps of $\sqrt{3}$ -subdivision. The scheme is numerically stable and generally applicable, there are no restrictions on the initial triangulation.

Keywords: Powell–Sabin splines, subdivision, normalised B-splines, CAGD

AMS(MOS) classification: 65D07, 65D17, 68U07

1 Introduction

Geometric modelling of complex shapes heavily relies on the use of powerful mathematical representations of surfaces. Widely used now in CAGD packages is the tensor product B-spline representation, which is, however, restricted to rectangular domains, and therefore is not well suited for designing surfaces with an arbitrary number of edges. Farins Bézier triangles [2] are a worthwhile alternative to represent piecewise polynomials on polygonal domains, but imposing smoothness conditions between the patches requires a great number of nontrivial relations between the coefficients to be satisfied. Another approach is a B-spline representation for Powell–Sabin (PS)-splines by Shi *et al.* [6], but their construction method has some serious drawbacks from the numerical point of view. Dierckx [1] presented an improved algorithm to construct a normalised B-spline basis for PS-splines, which guarantees global C^1 smoothness for any choice of the coefficients, and resolves the numerical problems. This representation also has a nice geometric interpretation involving tangent control triangles for manipulating the PS-surfaces.

For the graphical display of a surface we need a denser set of points that represent the surface, or in other words, we need a representation of the surface on a refinement of the triangulation on which it is defined. This procedure is called subdivision. Because after subdivision the new basis functions have smaller support, it also gives the designer more local control when manipulating surfaces. Windmolders and Dierckx [8] solved the subdivision problem for uniform Powell–Sabin splines, that is on triangulations with all equilateral triangles. In this paper we solve the subdivision problem for general Powell–Sabin splines.

Section 2 recalls some general concepts of polynomials on triangulations and gives the definition of the space of Powell–Sabin splines. It also covers the relevant aspects of the construction of a normalised B-spline basis. Section 3 first gives an overview of possible subdivision schemes. Then the subdivision rules are developed for the case of triadic subdivision. The boundaries are treated separately. Finally we conclude with some remarks and suggestions for further research in section 5.

2 Powell–Sabin splines

2.1 Polynomials on triangles

Let $\lambda = (\lambda_1, \lambda_2, \lambda_3)$, $|\lambda| = \lambda_1 + \lambda_2 + \lambda_3 = d$, $\lambda_i \in \{0, 1, \dots, d\}$ using standard multi index notation. Consider a non degenerate triangle $\mathcal{T}(T_1, T_2, T_3)$ in a plane with its vertices having Cartesian coordinates $T_i(x_i, y_i)$, $i = 1, 2, 3$. Any point $P(x, y)$ in that plane can be expressed in terms of barycentric coordinates $\tau = (\tau_1, \tau_2, \tau_3)$ with respect to \mathcal{T} : $P = \sum_{i=1}^3 \tau_i T_i$ where $|\tau| = 1$. These barycentric coordinates are the unique solution to the system

$$\begin{bmatrix} x_1 & x_2 & x_3 \\ y_1 & y_2 & y_3 \\ 1 & 1 & 1 \end{bmatrix} \begin{bmatrix} \tau_1 \\ \tau_2 \\ \tau_3 \end{bmatrix} = \begin{bmatrix} x \\ y \\ 1 \end{bmatrix}. \quad (2.1)$$

A Bézier polynomial [2] of degree d over the triangle \mathcal{T} is defined by

$$b_{\mathcal{T}}^d(P) = b_{\mathcal{T}}^d(\tau) = \sum_{|\lambda|=d} b_{\lambda} B_{\lambda}^d(\tau), \quad (2.2)$$

in which b_{λ} are called Bézier ordinates, and

$$B_{\lambda}^d(\tau) = \frac{d!}{\lambda_1! \lambda_2! \lambda_3!} \tau_1^{\lambda_1} \tau_2^{\lambda_2} \tau_3^{\lambda_3} \quad (2.3)$$

are the Bernstein–Bézier polynomials on the triangle.

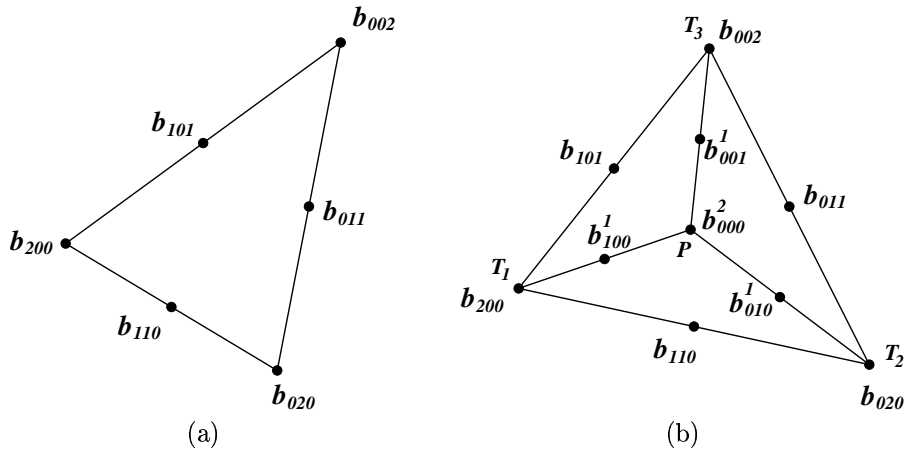


Figure 1. (a) Positions of Bézier ordinates for $d = 2$. (b) The de Casteljau algorithm for evaluating a polynomial at a point P gives the Bézier ordinates of that polynomial on the triangles (T_1, T_2, P) , (T_1, P, T_3) and (P, T_2, T_3) .

The points $(\frac{\lambda}{d}, b_{\lambda})$ are the control points for the surface $z = b_{\mathcal{T}}^d(\tau)$ and the piecewise linear interpolant to these points is the Bézier net or control net. This is displayed schematically in figure 1(a) for the case $d = 2$. The points $\frac{\lambda}{d}$, marked with dots on the figure, are called Bézier triangle points.

Polynomials in their Bernstein–Bézier representation (2.2) can be evaluated efficiently using the de Casteljau algorithm

$$b_{\mathcal{T}}^d(\tau) = b_{000}^d(\tau) \quad (2.4)$$

with

$$\begin{aligned} b_{ijk}^0(\tau) &= b_{ijk}, \\ b_{ijk}^r(\tau) &= \tau_1 b_{(i+1)jk}^{r-1}(\tau) + \tau_2 b_{i(j+1)k}^{r-1}(\tau) + \tau_3 b_{ij(k+1)}^{r-1}(\tau), \quad r = 1, \dots, d, \quad i + j + k + r = d. \end{aligned} \quad (2.5)$$

The de Casteljau algorithm has several interesting properties and consequences.

(1) *Subdivision*

It gives directly the Bézier ordinates of the given polynomial with respect to the triangles (T_1, T_2, P) , (T_1, P, T_3) and (P, T_2, T_3) where P is the point in which the polynomial is evaluated. This is illustrated in figure 1(b) for the case $d = 2$.

(2) *Continuity*

Continuity conditions between triangles can be expressed as relations between the Bézier ordinates. Let $b_{\mathcal{T}}^d(\tau)$ a polynomial with Bézier ordinates b_{ijk} on the triangle $\mathcal{T}(T_1, T_2, T_3)$, and $c_{\mathcal{T}^*}^d(\tau)$ a polynomial with Bézier ordinates c_{ijk} on the triangle $\mathcal{T}^*(T_1^*, T_2, T_3)$ where T_1^* has barycentric coordinates λ with respect to $\mathcal{T}(T_1, T_2, T_3)$. A necessary and sufficient condition for $b_{\mathcal{T}}^d(\tau)$ and $c_{\mathcal{T}^*}^d(\tau)$ to be C^r continuous across the common boundary is

$$c_{ijk} = b_{0jk}^i(\lambda), \quad i = 0, 1, \dots, r, \quad i + j + k = d. \quad (2.6)$$

In the case of C^1 continuity this becomes

$$C^0 : c_{0jk} = b_{0jk}, \quad (2.7)$$

$$C^1 : c_{1jk} = \lambda_1 b_{1jk} + \lambda_2 b_{0(j+1)k} + \lambda_3 b_{0j(k+1)}. \quad (2.8)$$

(3) *Tangent property*

The control net mimics the shape of the surface and is tangent to the polynomial surface at the three vertices of the triangle.

Representing complex shapes, however, requires to use patch complexes with a great number of Bézier triangles. Keeping up continuity conditions between all the neighbouring patches then results, in general, in nontrivial relations between their Bézier ordinates. The use of split triangles can overcome this problem.

2.2 PS–splines

Consider a simply connected subset $\Omega \subset \mathbb{R}^2$ with polygonal boundary $\delta\Omega$. Suppose we have a conforming triangulation Δ of Ω , being constituted of triangles ρ_j , $j = 1, \dots, t$, and having vertices V_k with Cartesian coordinates (x_k, y_k) , $k = 1, \dots, n$. Let Δ^* be a Powell–Sabin refinement of Δ , which divides each triangle ρ_j into six smaller triangles with a common vertex Z_j as follows (figure 2) :

- (1) Choose an interior point Z_j in each triangle ρ_j , so that if two triangles ρ_i and ρ_j have a common edge, then the line joining these interior points Z_i and Z_j intersects the common edge at a point R_{ij} between its vertices. Choosing Z_j as the incentre of each triangle ρ_j ensures the existence of the points R_{ij} . Other choices may be more appropriate from the practical point of view.

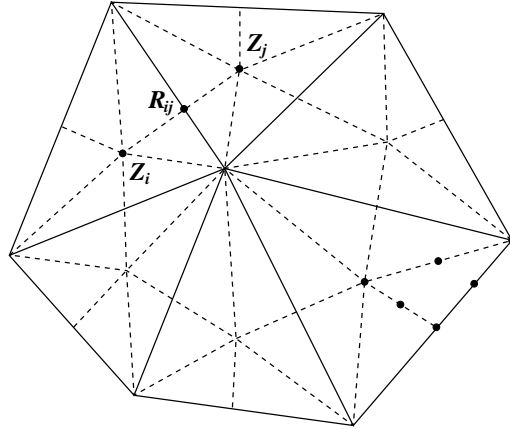


Figure 2. PS-refinement. Each triangle ρ_j is split into six smaller triangles with a common vertex Z_j .

- (2) Join each point Z_j to the vertices of ρ_j .
- (3) For each edge of the triangle ρ_j
 - which belongs to the boundary $\delta\Omega$, join Z_j to an arbitrary point of the edge.
 - which is common to a triangle ρ_i , join Z_j to R_{ij} .

Now we consider the space of piecewise C^1 continuous quadratic polynomials on Δ^* , the Powell–Sabin splines. It is denoted by $S_2^1(\Delta^*)$. Each of the $6t$ triangles resulting from the PS-refinement becomes the domain triangle of a quadratic Bernstein–Bézier polynomial, i.e. we choose $d = 2$ in equation (2.2) and (2.3), as indicated for one subtriangle in figure 2. Powell and Sabin [5] proved that the dimension of the space $S_2^1(\Delta^*)$ equals $3n$: there exists a unique solution $s(x, y) \in S_2^1(\Delta^*)$ for the interpolation problem

$$s(V_k) = f_k, \quad \frac{\partial s}{\partial x}(V_k) = f_{x,k}, \quad \frac{\partial s}{\partial y}(V_k) = f_{y,k}, \quad k = 1, \dots, n. \quad (2.9)$$

So given the function and derivative values at each vertex V_k , the Bézier ordinates on the domain subtriangles are uniquely defined and the continuity conditions between subtriangles are automatically fulfilled.

2.3 A normalised B-spline representation

Dierckx [1] showed that each piecewise polynomial $s(x, y) \in S_2^1(\Delta^*)$ has a unique representation

$$s(x, y) = \sum_{i=1}^n \sum_{j=1}^3 c_{ij} B_i^j(x, y), \quad (x, y) \in \Omega, \quad (2.10)$$

where the basis functions satisfy

$$B_i^j(x, y) \geq 0 \quad (2.11)$$

$$\sum_{i=1}^n \sum_{j=1}^3 B_i^j(x, y) \equiv 1, \quad (2.12)$$

and have local support: $B_i^j(x, y)$ is nonzero only on the so-called molecule M_i of V_i , being the set of triangles ρ_l that have V_i as a vertex. The number of triangles in M_i is called the molecule number m_i .

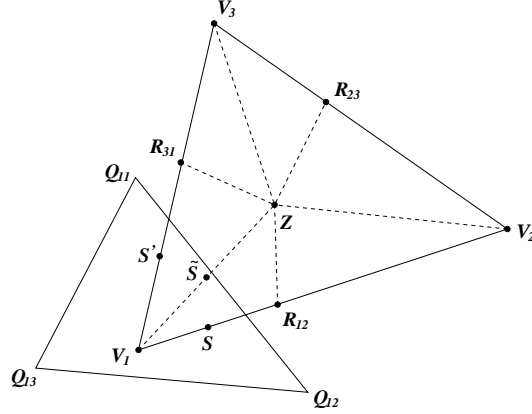


Figure 3: PS-points and PS-triangle.

To construct the basis functions $B_i^j(x, y)$ we use the algorithm from [1].

- (1) For each vertex $V_i \in \Delta$, identify its PS-points. This is a number of particular surrounding Bézier triangle points and the vertex V_i itself. Figure 3 shows the PS-points S, \tilde{S}, S' and V_1 for the vertex V_1 in the triangle $\rho(V_1, V_2, V_3)$.
- (2) For each vertex V_i , find a triangle $t_i(Q_{i1}, Q_{i2}, Q_{i3})$ containing all the PS-points of V_i (from all the triangles ρ_l in the molecule M_i). Denote its vertices $Q_{ij}(X_{ij}, Y_{ij})$. The triangles $t_i, i = 1, \dots, n$ are called PS-triangles. Figure 3 also shows such a PS-triangle t_1 .

We denote the barycentric coordinates of the PS-points S_i, \tilde{S}_i and S'_i with respect to the triangle $t_i(Q_{i1}, Q_{i2}, Q_{i3})$ with $(L_{i1}, L_{i2}, L_{i3}), (\tilde{L}_{i1}, \tilde{L}_{i2}, \tilde{L}_{i3})$ and $(L'_{i1}, L'_{i2}, L'_{i3})$.

- (3) Given the PS-triangle t_i of a vertex V_i , three linearly independent triplets of real numbers can be found as follows:

$$\alpha_i = (\alpha_{i1}, \alpha_{i2}, \alpha_{i3}) \text{ are the barycentric coordinates of } V_i \text{ with respect to } t_i, \quad (2.13)$$

$$\beta_i = (\beta_{i1}, \beta_{i2}, \beta_{i3}) = \left(\frac{Y_{i2} - Y_{i3}}{e}, \frac{Y_{i3} - Y_{i1}}{e}, \frac{Y_{i1} - Y_{i2}}{e} \right) \quad (2.14)$$

$$\gamma_i = (\gamma_{i1}, \gamma_{i2}, \gamma_{i3}) = \left(\frac{X_{i3} - X_{i2}}{e}, \frac{X_{i1} - X_{i3}}{e}, \frac{X_{i2} - X_{i1}}{e} \right), \quad (2.15)$$

where

$$e = \begin{vmatrix} X_{i1} & Y_{i1} & 1 \\ X_{i2} & Y_{i2} & 1 \\ X_{i3} & Y_{i3} & 1 \end{vmatrix}. \quad (2.16)$$

We have $|\alpha_i| = 1$ and $|\beta_i| = |\gamma_i| = 0$.

- (4) The basis function $B_i^j(x, y)$ is the unique solution of the interpolation problem (2.9) with all $(f_k, f_{x,k}, f_{y,k}) = (0, 0, 0)$ except for $(f_i, f_{x,i}, f_{y,i}) = (\alpha_{ij}, \beta_{ij}, \gamma_{ij})$.

We define the control points as

$$C_{ij} = (Q_{ij}, c_{ij}) = (X_{ij}, Y_{ij}, c_{ij}) \quad (2.17)$$

and the control triangles as

$$T_i(C_{i1}, C_{i2}, C_{i3}). \quad (2.18)$$

The projection of the control triangles T_i in the (x, y) plane are the PS–triangles t_i . One can prove that the control triangle T_i is tangent to the surface $z = s(x, y)$ at V_i . The tangent point is $(x_i, y_i, s(V_i))$.

The fact that the PS–triangle t_i contains the PS–points of the vertex V_i guarantees property (2.11). For design purposes we prefer the control points of the corresponding control triangle to be close to the surface. In [1] the PS–triangle with the smallest area is computed, but other choices are possible.

2.4 Bézier representation of a PS–spline

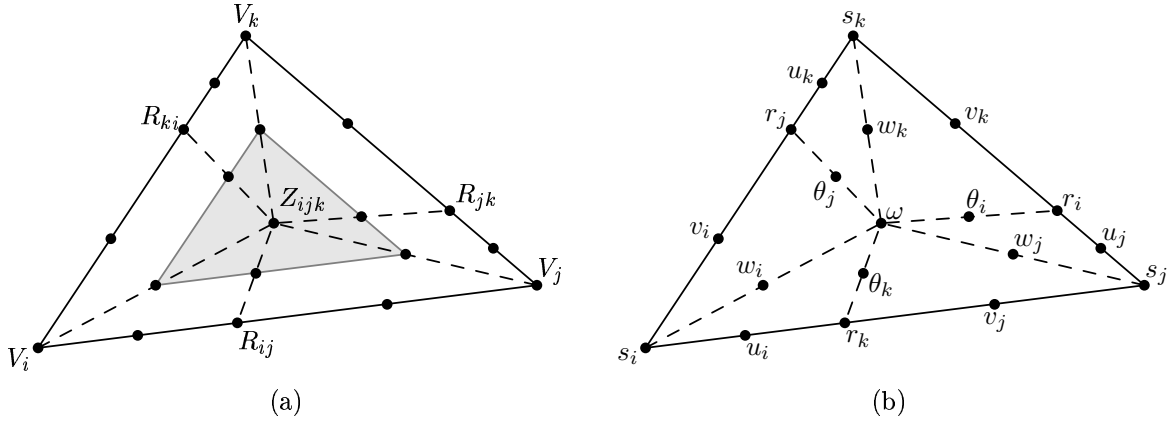


Figure 4. (a) PS–refinement of a triangle $\rho(V_i, V_j, V_k)$. (b) Schematic representation of Bézier ordinates.

The Bézier representation of a PS–spline surface can be calculated from the B–spline representation. Consider a domain triangle $\rho(V_i, V_j, V_k) \in \Delta$ with its PS–refinement on figure 4(a), where

$$\begin{aligned} R_{ij} &= \lambda_{ij}V_i + (1 - \lambda_{ij})V_j \\ R_{jk} &= \lambda_{jk}V_j + (1 - \lambda_{jk})V_k \\ R_{ki} &= \lambda_{ki}V_k + (1 - \lambda_{ki})V_i \\ Z_{ijk} &= a_{ijk}V_i + b_{ijk}V_j + c_{ijk}V_k. \end{aligned} \quad (2.19)$$

Denote the Bézier ordinates as on figure 4(b). They can be written as the following unique convex barycentric combinations of the B–spline coefficients:

$$\begin{aligned} s_i &= \alpha_{i1}c_{i1} + \alpha_{i2}c_{i2} + \alpha_{i3}c_{i3} \\ u_i &= L_{i1}c_{i1} + L_{i2}c_{i2} + L_{i3}c_{i3} \\ v_i &= L'_{i1}c_{i1} + L'_{i2}c_{i2} + L'_{i3}c_{i3} \\ w_i &= \tilde{L}_{i1}c_{i1} + \tilde{L}_{i2}c_{i2} + \tilde{L}_{i3}c_{i3}. \end{aligned} \quad (2.20)$$

The coefficients in these formulae depend on the geometry of the PS–refinement, and on the choice of the PS–triangles. Similar expressions hold for (s_j, u_j, v_j, w_j) and (s_k, u_k, v_k, w_k) . The other Bézier

ordinates can be found from the C^1 continuity conditions (2.7) and (2.8), e.g.,

$$\begin{aligned} r_k &= \lambda_{ij}u_i + (1 - \lambda_{ij})v_j \\ \theta_k &= \lambda_{ij}w_i + (1 - \lambda_{ij})w_j \\ \omega &= a_{ijk}w_i + b_{ijk}w_j + c_{ijk}w_k. \end{aligned} \tag{2.21}$$

Consider the triangle $T_{ijk}^{\sqrt{3}}$ formed by the Bézier control points corresponding to the Bézier ordinates w_i , w_j and w_k . The specific notation with the superscript $\sqrt{3}$ will be clarified later. From the tangent property of the Bézier control net for each of the Bézier triangles in the PS-refinement follows that $T_{ijk}^{\sqrt{3}}$ is tangent to the surface at $(Z_{ijk}, w = s(Z_{ijk}))$. Notice that also the Bézier control points corresponding to θ_i , θ_j and θ_k lie in $T_{ijk}^{\sqrt{3}}$. The projection of $T_{ijk}^{\sqrt{3}}$ in the (x,y) plane, $t_{ijk}^{\sqrt{3}}$, will also be used in the next sections and is shaded in figure 4(a).

3 Subdivision

The goal of subdivision is to calculate the B-spline representation (2.10) of a PS-spline surface on a refinement Δ^1 of the given triangulation Δ^0 . The new basis functions after subdivision have smaller support and give the designer more local control when manipulating surfaces. Adjusting one coefficient c_{ij} of a control point of a subdivided PS-spline surface, influences a smaller neighbourhood of the involved vertex. The control triangles are tangent to the surface and in case of repeated subdivision, the linear interpolant of the tangent points converges to the surface itself. Therefore subdivision is a common technique for displaying surfaces graphically.

In section 3.1 we consider different possibilities for the refinement Δ^1 of the original triangulation Δ^0 . This answers the question where to place the new vertices. Then, in section 3.2, we derive the subdivision rules for the triadic case. For each new vertex we first determine a valid PS-triangle by requesting that it contains all its PS-points. Then we find the control points of the corresponding control triangle in terms of the old control points.

3.1 Choosing a suitable refinement Δ^1 of Δ^0

3.1.1 Dyadic subdivision

The most obvious possibility is dyadic subdivision. In this scheme a new vertex is inserted on every edge between two old vertices and every original triangle is split into four new triangles.

- (1) In the first step we choose the positions of the new vertices. The lines of the PS-refinement Δ^{0*} of the initial triangulation Δ^0 must be maintained in the PS-refinement Δ^{1*} of the refined triangulation Δ^1 because the aim is to represent exactly the same surface. To ensure this, the new vertices have to be placed on the intersections R_{ij} of the lines of the PS-refinement $Z_{ijk}R_{ij}$ with the edges V_iV_j . This step is illustrated in figure 5.
- (2) In the second step we determine the PS-refinement Δ^{1*} for each of the four new triangles. For the triangle (V_{ij}, V_{jk}, V_{ki}) the PS-refinement is already fixed, the point Z_{ijk} is the interior point for this triangle. The interior points for the three remaining triangles have to lie on the line of the old PS-refinement Δ^{0*} that crosses the new triangle. This step is illustrated in figure 6.

The dyadic scheme was used by Windmolders and Dierckx for uniform Powell-Sabin splines, this is on a triangulation with all equilateral triangles. The subdivision rules for this special case can be found in [8]. In the general case the idea of dyadic subdivision can only be used under certain

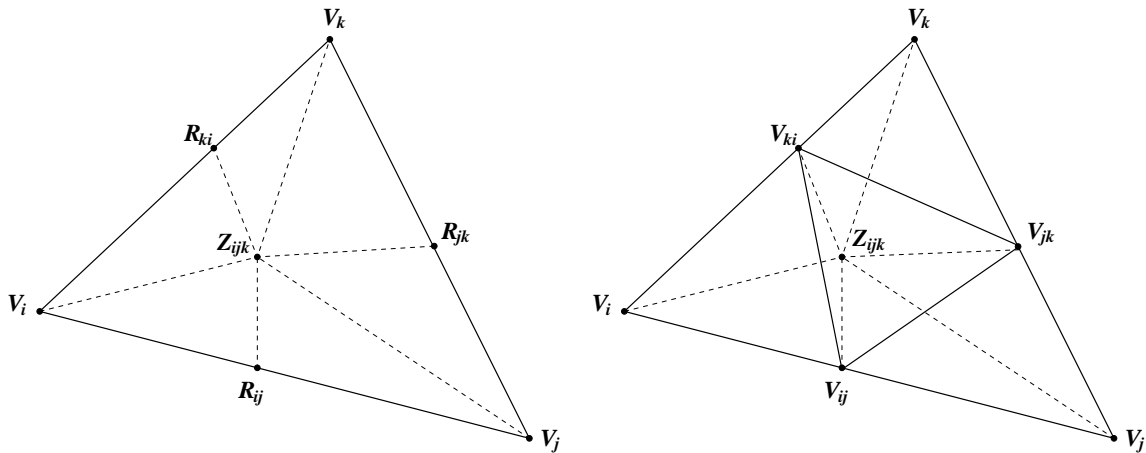


Figure 5. Principle of dyadic subdivision. In the first step we place the new vertices on the intersection of the lines of the PS-refinement with the edges.

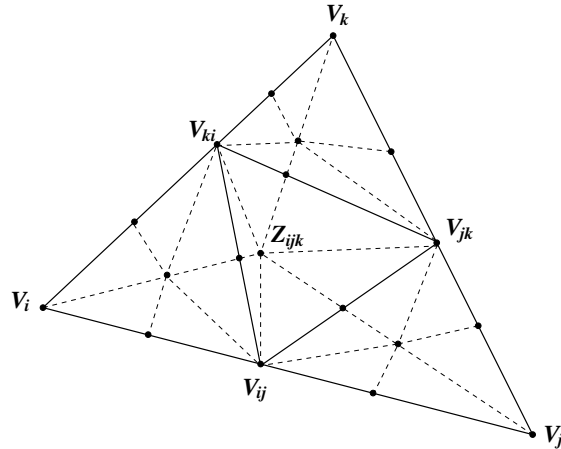


Figure 6. Principle of dyadic subdivision. In the second step we determine a PS-refinement for each of the four new triangles.

conditions. For example, the point Z_{ijk} of the PS-refinement of a triangle, must lie inside the middle triangle $(V_{ij}V_{jk}V_{ki})$. This leads to conditions on the initial triangulation Δ^0 and its PS-refinement Δ^{0*} , i.e. on the placement of the interior points Z_{ijk} and the resulting positions of the R_{ij} : the dyadic scheme is not generally applicable.

3.1.2 Triadic subdivision

Another possibility is triadic subdivision. In this scheme every edge is split in 3 instead of 2 and every original triangle is split into nine new triangles.

- (1) In the first step we choose the positions of the new vertices. Two new vertices are inserted on every edge and one new vertex is added inside each triangle. Because of the same reasoning as in the dyadic case, the new vertex inside the triangle must coincide with the interior point

Z_{ijk} , and the new vertices on the edges must lie each at one side of the points R_{ij} :

$$\begin{aligned} V_{ij} &= \omega_{ij}V_i + (1 - \omega_{ij})R_{ij} \\ V_{ji} &= \omega_{ji}V_j + (1 - \omega_{ji})R_{ij} \\ V_{ijk} &= Z_{ijk}. \end{aligned} \tag{3.1}$$

In these formulas ω_{ij} and ω_{ji} have a value between 0 and 1

$$0 < \omega_{ij}, \omega_{ji} < 1. \tag{3.2}$$

This step is illustrated in figure 7.

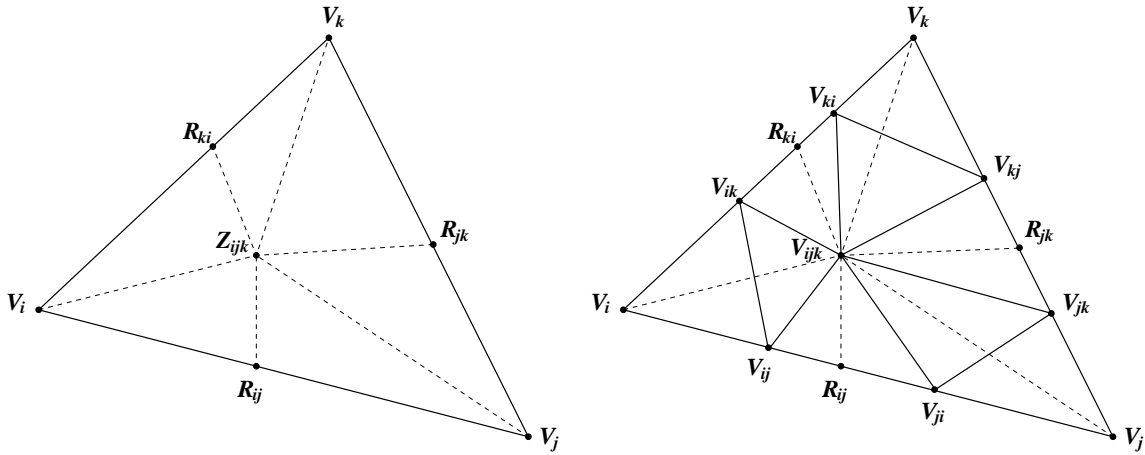


Figure 7. Principle of triadic subdivision. In the first step we place a new vertex at the position of the interior point Z_{ijk} and two new vertices on the edges each at one side of the R_{ij} .

For the resulting refinement to exist, the interior point Z_{ijk} has to lie inside the hexagon formed by the new vertices $(V_{ij}, V_{ji}, V_{jk}, V_{kj}, V_{ki}, V_{ik})$ as shown in figure 8. It is always possible to place these new vertices, i.e. choose a value for the ω in equation (3.1), such that this condition is fulfilled: there are no conditions on the initial triangulation Δ^0 or its PS-refinement Δ^{0*} . Therefore we prefer to use the triadic scheme instead of the dyadic scheme to develop subdivision rules for general Powell–Sabin splines.

- (2) In the second step we determine the PS-refinement Δ^{1*} for each of the nine new triangles. Each new interior point has to lie on the line of the old PS-refinement Δ^{0*} that crosses the new triangle. This step is illustrated in figure 9.

3.2 Calculating the refined B-spline representation

3.2.1 $\sqrt{3}$ -subdivision

Triadic subdivision can also be seen as two steps of the so called $\sqrt{3}$ -subdivision scheme. This kind of scheme was first introduced by Kobbelt [3] and Labsik and Greiner[4] and used for uniform Powell–Sabin splines by Vanraes *et al.* [7]. The new triangulation $\Delta^{\sqrt{3}}$ is constructed by inserting a new vertex V_{ijk} at the position of the interior point Z_{ijk} of each triangle. Except at the boundaries,

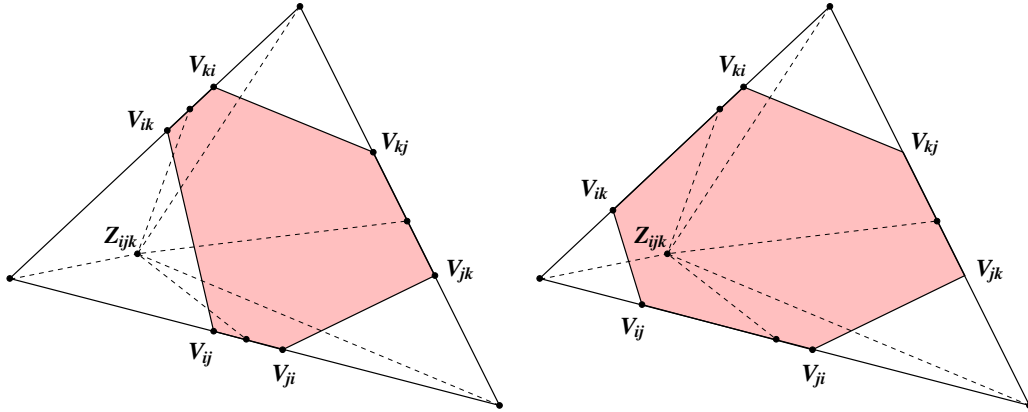


Figure 8. (a) Z_{ijk} does not lie inside the hexagon formed by $(V_{ij}, V_{ji}, V_{jk}, V_{kj}, V_{ki}, V_{ik})$: the refinement is not valid. (b) A valid placement for the new vertices in triadic subdivision always exists. There are no conditions on the initial triangulation.

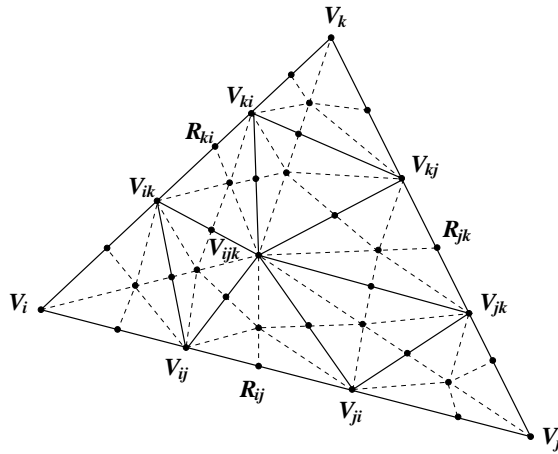


Figure 9. Principle of triadic subdivision. In the second step we determine a PS-refinement for each of the nine new triangles.

the old edges are not preserved in the new triangulation. Instead new edges are introduced connecting every new vertex V_{ijk} with the vertices of the old triangle it lies in, and connecting every two new vertices that lie in neighbouring old triangles. Figure 10(b) shows the result of $\sqrt{3}$ -subdivision on the triangulation Δ^0 of figure 10(a). In this figures the PS-refinement is not shown, but remark that the new edges in $\Delta^{\sqrt{3}}$ must coincide with the lines of the PS-refinement Δ^{0*} and that the original edges of Δ^0 are now part of the new PS-refinement $\Delta^{\sqrt{3}*}$.

In the new triangles new interior points must be chosen on the one line of the new PS-refinement $\Delta^{\sqrt{3}*}$ that is already fixed, that is, the original edge that crosses the triangle. Applying the $\sqrt{3}$ -subdivision operator a second time, again results in new vertices that coincide with the interior points that in this case lie on the edges of the initial triangulation. As can be seen in figure 10(c), this causes a refinement with tri-section of every original edge and splitting of each original triangle into nine subtriangles. Hence one single refinement step of this scheme can be considered as the

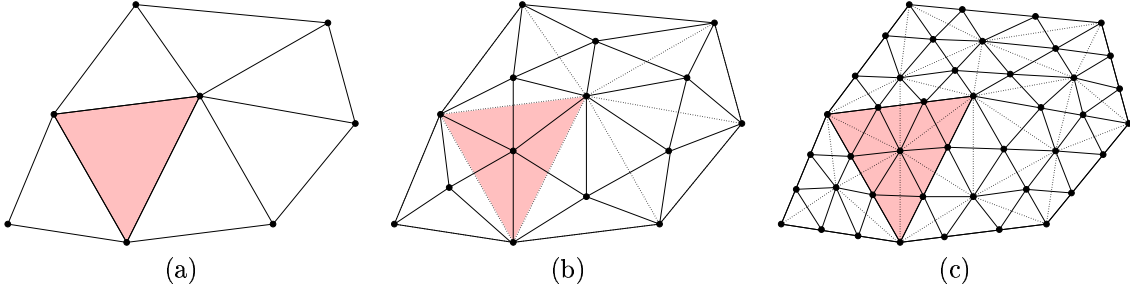


Figure 10. Principle of $\sqrt{3}$ -subdivision. Applying $\sqrt{3}$ -subdivision twice results in triadic subdivision. The PS-refinements are not shown.

square root of one step of the triadic scheme. If we look back at figure 9 with this knowledge of $\sqrt{3}$ -subdivision, we can see that the vertex V_{ijk} was added in the first step of $\sqrt{3}$ -subdivision, and the vertices V_{ij} were added in the second step of $\sqrt{3}$ -subdivision. The lines $V_i V_{ijk}$ and $V_{ijk} R_{ij}$ that are part of the PS-refinement of the initial triangulation, were edges after the first $\sqrt{3}$ -subdivision step and are now again part of the PS-refinement.

3.2.2 The triangles $t_{ijk}^{\sqrt{3}}$ and $T_{ijk}^{\sqrt{3}}$

We now show that, after one $\sqrt{3}$ -subdivision step, the triangles $T_{ijk}^{\sqrt{3}}$, introduced in the last paragraph of section 2.4, can act as control triangles for the new vertices V_{ijk} at the position of the Z_{ijk} . Recall that this triangle is defined by three particular Bézier control points as shown in figure 4(a). We denote these new control points with $C_{ijk,1}^{\sqrt{3}}$, $C_{ijk,2}^{\sqrt{3}}$ and $C_{ijk,3}^{\sqrt{3}}$. The corners of the corresponding PS-triangle $t_{ijk}^{\sqrt{3}}$ are then $Q_{ijk,1}^{\sqrt{3}}$, $Q_{ijk,2}^{\sqrt{3}}$ and $Q_{ijk,3}^{\sqrt{3}}$. From (2.20) we know that

$$\begin{aligned} C_{ijk,1}^{\sqrt{3}} &= \tilde{L}_{i1} C_{i1} + \tilde{L}_{i2} C_{i2} + \tilde{L}_{i3} C_{i3} \\ C_{ijk,2}^{\sqrt{3}} &= \tilde{L}_{j1} C_{j1} + \tilde{L}_{j2} C_{j2} + \tilde{L}_{j3} C_{j3} \\ C_{ijk,3}^{\sqrt{3}} &= \tilde{L}_{k1} C_{k1} + \tilde{L}_{k2} C_{k2} + \tilde{L}_{k3} C_{k3}. \end{aligned} \quad (3.3)$$

The same convex combinations also apply for $Q_{ijk}^{\sqrt{3}}$.

To prove that $T_{ijk}^{\sqrt{3}}$ is indeed a valid control triangle, we first need to prove that $t_{ijk}^{\sqrt{3}}$ is a valid PS-triangle, or in other words, that $t_{ijk}^{\sqrt{3}}$ contains all the involved PS-points after one step of $\sqrt{3}$ -subdivision.

Figure 11 shows one triangle $\rho(V_i, V_j, V_k)$ of the initial triangulation Δ^0 after one step of $\sqrt{3}$ -subdivision. In this triangle there is one new vertex V_{ijk} at the position of the interior point Z_{ijk} and the vertices V_{ij} and V_{ji} (that are introduced after a second $\sqrt{3}$ -subdivision step, but that are interior points for $\Delta^{\sqrt{3}}$ at this stage) are already marked on the figure. The molecule number m_{ijk} of V_{ijk} is always six and there are twelve PS-points, shown as gray dots, plus the vertex V_{ijk} itself, that have to be contained in the new PS-triangle. The proposed PS-triangle $t_{ijk}^{\sqrt{3}}$ is marked in gray. On this figure we can see that the corners $Q_{ijk}^{\sqrt{3}}$ of this triangle are PS-points of the original PS-refinement Δ^{0*} that lie on the new edges of $\Delta^{\sqrt{3}}$ between V_{ijk} and the old vertices, or in other words, in the middle between V_{ijk} and the old vertices. We now zoom in on the left bottom corner and check that the PS-points A , B and C of $\Delta^{\sqrt{3}*}$ are contained in the proposed PS-triangle $t_{ijk}^{\sqrt{3}}$.

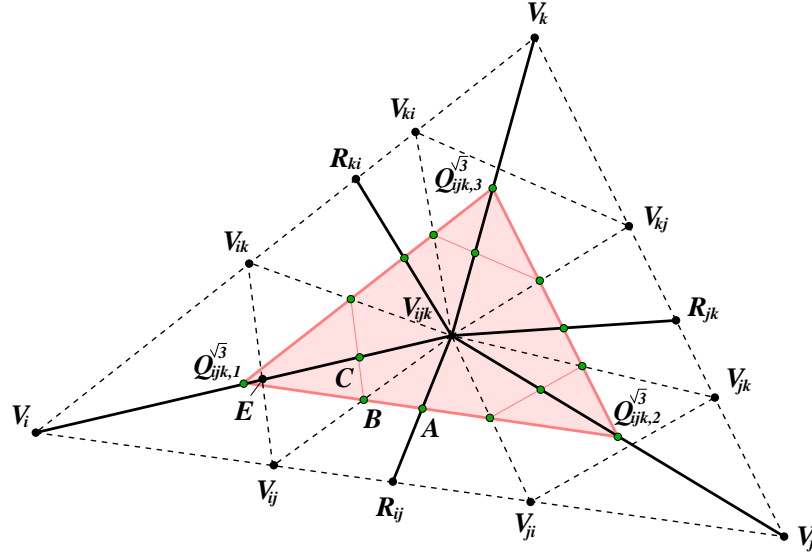


Figure 11. $t_{ijk}^{\sqrt{3}}$ is a valid PS-triangle for $V_{ijk} (= Z_{ijk})$ after one step of $\sqrt{3}$ -subdivision.

Referring to (2.19) and (3.1) it immediately follows that

$$A = \lambda_{ij} Q_{ijk,1}^{\sqrt{3}} + (1 - \lambda_{ij}) Q_{ijk,2}^{\sqrt{3}} \quad (3.4)$$

and

$$\begin{aligned} B &= \omega_{ij} Q_{ijk,1}^{\sqrt{3}} + (1 - \omega_{ij}) A \\ &= (\omega_{ij} + \lambda_{ij} - \omega_{ij} \lambda_{ij}) Q_{ijk,1}^{\sqrt{3}} + (1 - \lambda_{ij} - \omega_{ij} + \omega_{ij} \lambda_{ij}) Q_{ijk,2}^{\sqrt{3}}. \end{aligned} \quad (3.5)$$

Denote with E the intersection of $V_{ij}V_{ik}$ and $V_{ijk}V_i$. This is a point of the PS-refinement $\Delta^{\sqrt{3}*}$. We can determine $0 < r < 1$ such that

$$E = rV_i + (1 - r)V_{ijk}, \quad (3.6)$$

$$\begin{aligned} C &= \frac{1}{2}(E + V_{ijk}) \\ &= rQ_{(ijk)1}^{\sqrt{3}} + (1 - r)V_{ijk}, \\ &= ((1 - r)a_{ijk} + r)Q_{(ijk)1}^{\sqrt{3}} + (1 - r)b_{ijk}Q_{(ijk)2}^{\sqrt{3}} + (1 - r)c_{ijk}Q_{(ijk)3}^{\sqrt{3}}. \end{aligned} \quad (3.7)$$

From (3.4), (3.5) and (3.7) we see that the barycentric coordinates of A , B and C with respect to $t_{ijk}^{\sqrt{3}}$ are all positive, which means that they lie inside or on the boundary of the triangle $t_{ijk}^{\sqrt{3}}$. This is independent of the value for ω_{ij} that was used in equation (3.1) to determine the position of the new vertex V_{ij} , which in this case takes the role of interior point. The same reasoning can be used for the remaining PS-points of V_{ijk} and we conclude that $t_{ijk}^{\sqrt{3}}$ is a valid PS-triangle for the vertex V_{ijk} after one $\sqrt{3}$ -subdivision step.

For the corresponding triangle $T_{ijk}^{\sqrt{3}}$ to be a valid control triangle, it needs to be tangent to the surface at V_{ijk} . This follows from the tangent property of the Bézier control net as already mentioned in section 2.4.

3.2.3 Two steps of $\sqrt{3}$ -subdivision

We now use this knowledge of $\sqrt{3}$ -subdivision to develop subdivision rules for triadic subdivision. In the first $\sqrt{3}$ -step the vertex V_{ijk} is added. For this vertex we can use the PS-triangle $t_{ijk}^{\sqrt{3}}$. For the old vertices V_i we can reuse their PS-triangles t_i . The PS-points in $\Delta^{\sqrt{3}*}$ are now closer to V_i compared to the PS-points in Δ^{0*} and are therefore again inside this triangle.

The formulas (3.3) for this step, use only convex combinations of the old data. The barycentric coordinates \tilde{L} have values between 0 and 1. This means that this step is numerically stable.

In the second $\sqrt{3}$ -step the vertices V_{ij} and V_{ji} are added. To find valid PS-triangles for these vertices, we use exactly the same idea as in the first $\sqrt{3}$ -step. The corners of the new PS-triangle t_{ij} for V_{ij} are now the PS-points in $\Delta^{\sqrt{3}*}$ that lie in the middle between V_{ij} and its surrounding old vertices. For the old vertices, so both the V_i and the V_{ijk} introduced in the first step, we can reuse their PS-triangles.

Because we use the same principle as in the first step, we again use only convex combinations of the previous level, which in this case is $\Delta^{\sqrt{3}}$. Therefore the second $\sqrt{3}$ -step is also numerically stable. In the next subsection we take a closer look at the convex combinations used in the second step.

3.2.4 New vertices V_{ij} and V_{ji}

Figure 12 shows the old PS-triangles t_i and t_j in V_i and V_j , the intermediate PS-triangles $t_{ijk}^{\sqrt{3}}$ and $t_{ijk'}^{\sqrt{3}}$, and the resulting new PS-triangle t_{ij} for V_{ij} .

The corners Q_{ij} of t_{ij} coincide with the PS-points of the intermediate triangulation $\Delta^{\sqrt{3}}$ that lie in the middle between V_{ij} and the surrounding vertices. This means that the first corner $Q_{ij,1}$ coincides with the intermediate PS-point B between V_{ij} and V_{ijk} in figure 12. Referring to (3.5) and from the properties of the Bézier control net it follows that

$$C_{ij,1} = (\omega_{ij} + \lambda_{ij} - \omega_{ij}\lambda_{ij})C_{ijk,1}^{\sqrt{3}} + (1 - \omega_{ij} - \lambda_{ij} + \omega_{ij}\lambda_{ij})C_{ijk,2}^{\sqrt{3}}. \quad (3.8)$$

We can easily check that again this is a convex combination of data on the previous level since

$$\begin{aligned} \omega_{ij} + \lambda_{ij} - \omega_{ij}\lambda_{ij} &= \omega_{ij}(1 - \lambda_{ij}) + \lambda_{ij} > 0 \\ &= 1 - (1 - \omega_{ij})(1 - \lambda_{ij}) < 1. \end{aligned} \quad (3.9)$$

This conclusion can also be drawn directly from the geometry because $Q_{ij,1}$ lies inside the triangle $t_{ijk}^{\sqrt{3}}$ on the line between $Q_{ijk,1}^{\sqrt{3}}$ and $Q_{ijk,1}^{\sqrt{3}}$.

For $C_{ij,2}$ we find analogously

$$C_{ij,2} = (\omega_{ij} + \lambda_{ij} - \omega_{ij}\lambda_{ij})C_{ijk',1}^{\sqrt{3}} + (1 - \omega_{ij} - \lambda_{ij} + \omega_{ij}\lambda_{ij})C_{ijk',2}^{\sqrt{3}}. \quad (3.10)$$

The third corner $Q_{ij,3}$ of the new PS-triangle t_{ij} for V_{ij} coincides with the intermediate PS-point of $\Delta^{\sqrt{3}*}$ that lies in the middle of V_i and V_{ij} . Let

$$S_i = \frac{1}{2}(V_i + R_{ij}) \quad (3.11)$$

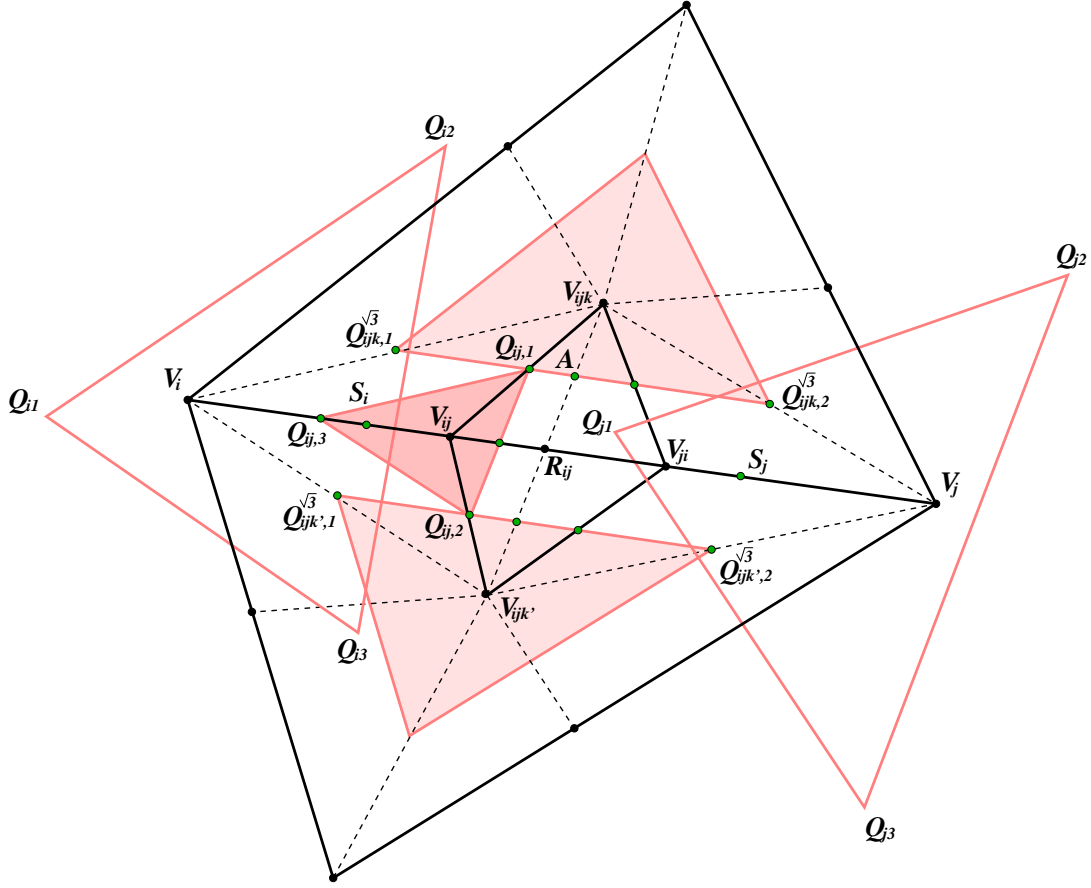


Figure 12: The PS-triangle for V_{ij} is found using two steps of $\sqrt{3}$ -subdivision.

a PS-point of Δ^{0*} , then according to (3.1) we have

$$\begin{aligned}
 Q_{ij,3} &= \frac{1}{2}(V_i + V_{ij}) \\
 &= \omega_{ij}V_i + (1 - \omega_{ij})S_i \\
 &= \omega_{ij}(\alpha_{i1}Q_{i1} + \alpha_{i2}Q_{i2} + \alpha_{i3}Q_{i3}) + (1 - \omega_{ij})(L_{i1}Q_{i1} + L_{i2}Q_{i2} + L_{i3}Q_{i3}) \\
 &= (L_{i1} + \omega_{ij}\alpha_{i1} - \omega_{ij}L_{i1})Q_{i1} + (L_{i2} + \omega_{ij}\alpha_{i2} - \omega_{ij}L_{i2})Q_{i2} \\
 &\quad + (L_{i3} + \omega_{ij}\alpha_{i3} - \omega_{ij}L_{i3})Q_{i3}.
 \end{aligned} \tag{3.12}$$

The coefficients in this combination are the barycentric coordinates of $Q_{ij,3}$ with respect to t_i . Since S_i is inside t_i , the same is true for $Q_{ij,3}$. Therefor (3.12) is also a convex combination of data on the previous level.

Again the same reasoning is valid for the corresponding control point

$$\begin{aligned}
 C_{ij,3} &= (L_{i1} + \omega_{ij}\alpha_{i1} - \omega_{ij}L_{i1})C_{i1} + (L_{i1} + \omega_{ij}\alpha_{i1} - \omega_{ij}L_{i2})C_{i2} \\
 &\quad + (L_{i2} + \omega_{ij}\alpha_{i3} - \omega_{ij}L_{i3})C_{i3}.
 \end{aligned} \tag{3.13}$$

Remark that these formulas are independent of the placement of the interior points in the nine new triangles after triadic subdivision. This was already mentioned in the proof that $T_{ijk}^{\sqrt{3}}$ can be used as a control triangle after one step of $\sqrt{3}$ -subdivision. Now we have used this idea twice to come to the formulas for triadic subdivision.

3.2.5 Boundaries

If the triangle (V_i, V_j, V_k) has no neighbouring triangle $(V_i, V_j, V_{k'})$, i.e. the edge $V_i V_j$ is a boundary edge, some of the subdivision rules found in the previous sections cannot be used. The formulas to find $t_{ijk}^{\sqrt{3}}$ remain valid. Only the equations to find the PS-triangles of the vertices V_{ij} and V_{ji} on the boundary use the data of the neighbouring triangle.

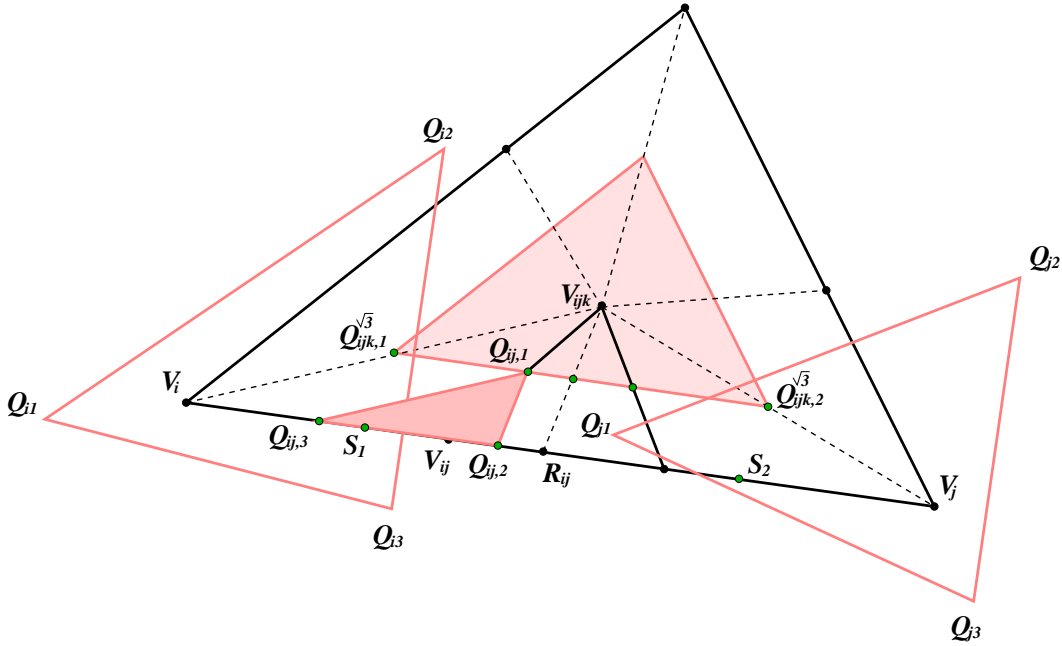


Figure 13. For vertices V_{ij} on a boundary edge we choose a different control triangle that only uses information of the triangle $(V_i V_j V_k)$.

More specific, equation (3.10) uses the points $Q_{ijk',1}^{\sqrt{3}}$ and $Q_{ijk',2}^{\sqrt{3}}$ which do not exist when $V_i V_j$ is a boundary edge. In this case we propose a different PS-triangle t_{ij} that uses only information of the triangle (V_i, V_j, V_k) . This is shown in figure 13.

$Q_{ij,2}$ now coincides with the point in the middle of V_{ij} and R_{ij} . Let

$$S_j = \frac{1}{2}(V_j + R_{ij}) \quad (3.14)$$

and S_i as in (3.11), then because of (2.19) and (3.1) we have

$$\begin{aligned}
Q_{ij,2} &= \omega_{ij}S_i + (1 - \omega_{ij})R_{ij} \\
&= \omega_{ij}S_i + (1 - \omega_{ij})(\lambda_{ij}S_i + (1 - \lambda_{ij})S_j) \\
&= (\omega_{ij} + \lambda_{ij} - \omega_{ij}\lambda_{ij})S_i + (1 - \omega_{ij} - \lambda_{ij} + \omega_{ij}\lambda_{ij})S_j \\
&= (\omega_{ij} + \lambda_{ij} - \omega_{ij}\lambda_{ij})(L_{i1}Q_{i1} + L_{i2}Q_{i2} + L_{i3}Q_{i3}) \\
&\quad + (1 - \omega_{ij} - \lambda_{ij} + \omega_{ij}\lambda_{ij})(L_{j1}Q_{j1} + L_{j2}Q_{j2} + L_{j3}Q_{j3}).
\end{aligned} \tag{3.15}$$

In this equation L_i and L_j are the barycentric coordinates of S_i and S_j with respect to t_i and t_j . The formulas for $Q_{ij,1}$ and $Q_{ij,2}$ remain unchanged, and again the same applies for the corresponding control points

$$\begin{aligned}
C_{ij,2} &= (\omega_{ij} + \lambda_{ij} - \omega_{ij}\lambda_{ij})(L_{i1}C_{i1} + L_{i2}C_{i2} + L_{i3}C_{i3}) \\
&\quad + (1 - \omega_{ij} - \lambda_{ij} + \omega_{ij}\lambda_{ij})(L_{j1}C_{j1} + L_{j2}C_{j2} + L_{j3}C_{j3}).
\end{aligned} \tag{3.16}$$

Remark that because of (3.9) this is a convex combination of the data on the previous level: the algorithm is also numerically stable at the boundaries.

4 Further optimisation

In the previous section we have solved the subdivision problem for general Powell–Sabin splines using the idea of $\sqrt{3}$ -subdivision. For the original vertices V_i we reused their PS-triangles. Also for the vertex V_{ijk} we reused the PS-triangle in the second $\sqrt{3}$ -step. This is a valid choice because after subdivision the PS-points are closer to the involved vertex and are therefore contained in the PS-triangle. In this section we suggest an optimisation for these vertices.

4.1 New vertices V_{ijk}

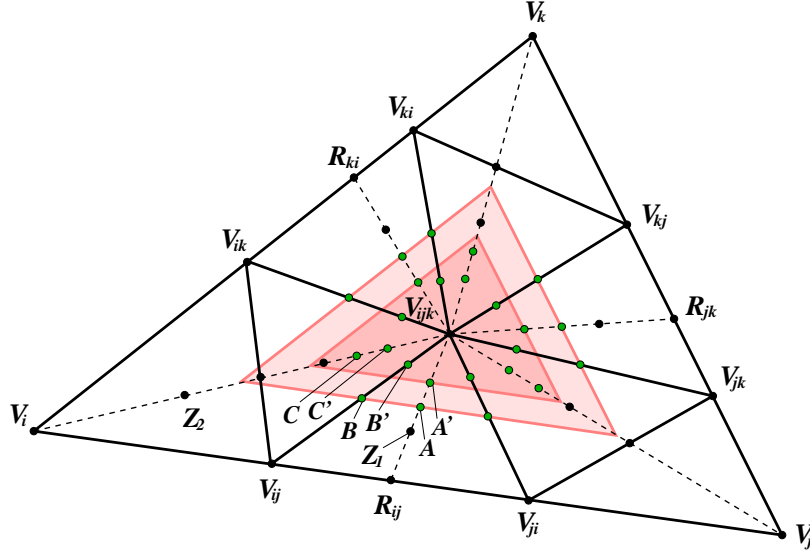


Figure 14. Rescaling the intermediate PS-triangle $t_{ijk}^{\sqrt{3}}$ gives a valid PS-triangle t_{ijk} for V_{ijk} .

We already know that $t_{ijk}^{\sqrt{3}}$ is a valid PS-triangle for V_{ijk} . It is however possible to choose a smaller PS-triangle, because after the second $\sqrt{3}$ -subdivision step the PS-points in Δ^{1*} are closer to V_{ijk} . Therefor we rescale $t_{ijk}^{\sqrt{3}}$ and denote the new PS-triangle with t_{ijk} .

To find the appropriate scaling factor, we need to know the positions of the interior points of the PS-refinement Δ^{1*} . For example for the new triangle $(V_{ij}, V_{ji}, V_{ijk})$ in figure 14, we choose the interior point Z_1 on the line of the original PS-refinement Δ^{0*} that crosses that triangle, that is between R_{ij} and V_{ijk}

$$Z_1 = \omega_{ijk}V_{ijk} + (1 - \omega_{ijk})R_{ij}, \quad 0 < \omega_{ijk} < 1 \quad (4.1)$$

and we suggest to choose the same value ω_{ijk} for the interior points of all six triangles that have V_{ijk} as a vertex. It is this value ω_{ijk} that we use to rescale $t_{ijk}^{\sqrt{3}}$, i.e.

$$Q_{ijk,1} = \omega_{ijk}(a_{ijk}Q_{ijk,1}^{\sqrt{3}} + b_{ijk}Q_{ijk,2}^{\sqrt{3}} + c_{ijk}Q_{ijk,3}^{\sqrt{3}}) + (1 - \omega_{ijk})Q_{ijk,1}^{\sqrt{3}}. \quad (4.2)$$

Rescaling A and C with ω_{ijk} with respect to V_{ijk} results in the PS-points A' and C' . It is obvious that these lie inside t_{ijk} . Because B' lies on the line between A' and C' this PS-point also lies inside t_{ijk} . The same reasoning can be used for the remaining PS-points, and this proves that all the PS-points lie inside the new triangle t_{ijk} . Therefor t_{ijk} is a valid PS-triangle for V_{ijk} after two steps of $\sqrt{3}$ -subdivision or one step of triadic subdivision.

Because $T_{ijk}^{\sqrt{3}}$ is tangent to the surface at V_{ijk} this is also the case for the rescaled version T_{ijk} and this is a valid control triangle for V_{ijk} . We can immediately write down the formulas for the new control points

$$\begin{aligned} C_{ijk,1} &= (1 - \omega_{ijk} + \omega_{ijk}a_{ijk})C_{ijk,1}^{\sqrt{3}} + \omega_{ijk}b_{ijk}C_{ijk,2}^{\sqrt{3}} + \omega_{ijk}c_{ijk}C_{ijk,3}^{\sqrt{3}} \\ C_{ijk,2} &= \omega_{ijk}a_{ijk}C_{ijk,1}^{\sqrt{3}} + (1 - \omega_{ijk} + \omega_{ijk}b_{ijk})C_{ijk,2}^{\sqrt{3}} + \omega_{ijk}c_{ijk}C_{ijk,3}^{\sqrt{3}} \\ C_{ijk,3} &= \omega_{ijk}a_{ijk}C_{ijk,1}^{\sqrt{3}} + \omega_{ijk}b_{ijk}C_{ijk,2}^{\sqrt{3}} + (1 - \omega_{ijk} + \omega_{ijk}c_{ijk})C_{ijk,3}^{\sqrt{3}}. \end{aligned} \quad (4.3)$$

4.2 New control triangles for old vertices V_i

Also for the old vertices V_i we can choose a smaller PS-triangle, though the old PS-triangle is still valid. The molecule number of these vertices is not necessarily six, but depends on the initial triangulation Δ^0 . After subdivision the molecule number remains the same in Δ^1 . In the surrounding new triangles we have not yet chosen a new interior point, which is necessary to find the scaling factor.

For example in figure 14 we choose the interior point Z_2 in triangle $(V_i V_j V_{ik})$ as

$$Z_2 = \omega_i V_i + (1 - \omega_i) V_{ik} \quad (4.4)$$

with

$$0 < r < \omega_j < 1. \quad (4.5)$$

The parameter r was used in (3.6) to define the point E in figure 11. This last requirement is to ensure that Z_2 lies in the triangle $(V_i V_j V_{ik})$ and not in the triangle $(V_{ij} V_{ik} V_{jk})$.

For the other new triangles that have V_i as a vertex that are not shown in the figure, we chose the same value ω_i , so that we can rescale the original control triangle with a factor ω_i with respect to V_i . The formulas for the new control points become

$$\begin{aligned} C'_{i1} &= (\omega_i \alpha_{i1} + 1 - \omega_i) C_{i1} + \omega_i \alpha_{i2} C_{i2} + \omega_i \alpha_{i3} C_{i3} \\ C'_{i2} &= \omega_i \alpha_{i1} C_{i1} + (\omega_i \alpha_{i2} + 1 - \omega_i) C_{i2} + \omega_i \alpha_{i3} C_{i3} \\ C'_{i3} &= \omega_i \alpha_{i1} C_{i1} + \omega_i \alpha_{i2} C_{i2} + (\omega_i \alpha_{i3} + 1 - \omega_i) C_{i3}. \end{aligned} \tag{4.6}$$

5 Concluding remarks

In this paper we have proposed an algorithm for computing the B-spline representation of a Powell-Sabin surface on a refinement of the given triangulation. We have chosen a triadic subdivision scheme because there are no restrictions on the initial triangulation, as opposed to a dyadic scheme. Triadic subdivision can be seen as two subsequent steps of $\sqrt{3}$ -subdivision. We developed the subdivision rules using the knowledge of control triangles on the intermediate level. For new vertices on the boundaries of the initial triangulation special rules apply. Since the algorithm uses only convex combinations it is numerically stable.

How to choose the parameters ω when placing the new vertices on the edges of the initial triangulation and the new interior points for the PS-refinement, is an open question. In most of the figures we have chosen $\omega = \frac{1}{3}$, because this leads to the expected refinement in case of equilateral triangles. However, this is not always possible, because V_{ijk} must be contained in the hexagon formed by $(V_{ij}V_{ji}V_{jk}V_{kj}V_{ki}V_{ik})$ and the new PS-refinement must exist.

For a triangulation with a certain PS-refinement, there are different possibilities for the control and PS-triangles. The only requirement is that a PS-triangle must contain all its PS-points. In [1] the control triangle with the smallest area is chosen, because then the control points are close to the surface. This leads to a quadratic programming problem. The control triangles of the new vertices V_{ij} and V_{ji} on the edges of the original triangulation are optimal in this sense. The scaling operation on the control triangles of the old vertices V_i also results in optimal triangles if the old control triangles were optimal, but the scaling on the intermediate control triangle for the interior vertices V_{ijk} results in control triangles that are not optimal. We are, however, sure that the control triangle shrinks in each step.

Wavelets can be developed with the technique of the lifting scheme with the subdivision scheme as the prediction step and an extra update step. This was already done for uniform Powell-Sabin splines in [9], but was not yet possible in the general case.

Acknowledgement

This work is partially supported by the Belgian Program on Interuniversity Poles of Attraction, initiated by the Belgian State, Prime Minister's Office for Science, Technology and Culture, and by the Flemish Fund for Scientific Research (FWO VLaanderen) project MISS (G.0211.02). The scientific responsibility rests with the authors.

Bibliography

1. P. Dierckx. On calculating normalized Powell-Sabin B-splines. *CAGD*, 15(3):61-78, 1997.
2. G. Farin. Triangular Bernstein-Bézier patches. *CAGD*, 3(2):83-128, 1986.

3. Leif Kobbelt. $\sqrt{3}$ -subdivision. In *Computer Graphics Proceedings*, Annual Conference Series. ACM SIGGRAPH, 2000.
4. U. Labsik and G. Greiner. Interpolatory $\sqrt{3}$ -subdivision. In Sabine Coquillart and Jr. Duke, David, editors, *Proceedings of the 21th European Conference on Computer Graphics (Eurographics-00)*, volume 19, 3 of *Computer Graphics Forum*, pages 131–138, Cambridge, August 21–25 2000. Blackwell Publishers.
5. M. J. D. Powell and M. A. Sabin. Piecewise quadratic approximations on triangles. *ACM Transactions on Mathematical Software*, 3:316–325, 1977.
6. X. Shi, S. Wang, W. Wang, and R. H. Wang. The C^1 quadratic spline space on triangulations. *Report 86004, Department of Mathematics, Jilin University, Changchun*, 1986.
7. E. Vanraes, J. Windmolders, A. Bultheel, and P. Dierckx. Dyadic and $\sqrt{3}$ -subdivision for Uniform Powell–Sabin splines. In *Information Visualisation Proceedings*. IEEE Computer Society, 2002.
8. J. Windmolders and P. Dierckx. Subdivision of Uniform Powell–Sabin splines. *CAGD*, 16:301–315, 1999.
9. J. Windmolders, E. Vanraes, P. Dierckx, and A. Bultheel. Uniform Powell–Sabin wavelets. TW Report 335, Department of Computer Science, Katholieke Universiteit Leuven, Belgium, February 2002.